Northwest Atlantic Fisheries Organization

Serial No. N6925 **NAFO SCR Doc. 19/010**

SCIENTIFIC COUNCIL MEETING – JUNE 2019

Biogeochemical oceanographic conditions in the Northwest Atlantic (NAFO subareas 2-3-4) during 2018

by

D. Bélanger[1], P. Pepin[1], G. Maillet[1], M. Blais[2], S. Plourde[2], B. Casault[3], C. Johnson[3], C. Caverhill[3], E. Devred[3]

[1] Fisheries and Oceans Canada, Northwest Atlantic Fisheries Centre, P.O. Box 5667, St. John's, NL, Canada, A1C 5X1

[2]Fisheries and Oceans Canada, Institut Maurice-Lamontagne, 850 Route de la mer, C.P. 1000, Mont-Joli, Qc,
[3]Fisheries and Oceans Canada, Bedford Institute of Oceanography, Box 1006, Dartmouth, NS, Canada, B2Y 4A2
Canada, G5H 3Z4

Abstract

Biological and chemical variables collected in 2018 from coastal high frequency monitoring stations and seasonal (spring, summer and fall) sampling of standard oceanographic sections covering the Newfoundland and Labrador Shelf (NAFO Subareas 2 and 3), the Grand Banks (Subareas 2 and 3), the Gulf of St. Lawrence (Subarea 4), the Scotian Shelf (Subarea 4) and the Gulf of Maine (Subarea 5) are presented and referenced to information from earlier periods when available. We review interannual variations in phytoplankton spring bloom indices (magnitude, initiation and duration) derived from satellite ocean colour imagery, as well as nitrate, chlorophyll *a* (chl *a*), and zooplankton abundance and biomass inventories collected as part of the 2018 Atlantic Zone Monitoring Program (AZMP). All time series are presented in standardized anomalies relative to a 1999-2015 climatology. In general, nitrate inventories in the upper (0-50 m) and lower (50-150 m) water column were near or below the climatology throughout the NW Atlantic in 2018 and presented respectively the second lowest and the lowest cumulated anomaly indices of the 20-y time series. The concentration of chl *a* in the first 100 m of the water column was near or above the climatology across the study area with the exception of the Bay of Fundy where a significant negative anomaly was observed. Chl *a* inventories in 2018 were higher than expected compared to either shallow, or 1-y lag deep nitrate concentrations considering the similar patterns of variation normally observed among these indices throughout the time series. Spring bloom indices derived from ocean colour satellite data indicated that the magnitude (total production) of the blooms was mainly near or below the climatology in most subregions. Blooms were later and slightly shorter than the climatology in the Labrador Sea and on the Labrador Shelf, earlier and longer than normal in most of the Gulf of St. Lawrence, and of normal timing and duration almost everywhere else. Spatial patterns in the abundance of copepod and non-copepod zooplankton in 2018 were similar to the previous year with above-normal abundances on the Newfoundland Shelf and the Grand Banks, and mainly near-normal abundances in the Gulf of St. Lawrence and on the Scotian Shelf with the exception of few negative copepod anomalies on the central and eastern Scotian Shelf. Overall copepod abundance in the NW Atlantic has decreased for a second consecutive year since the time-series record high observed in 2016, reaching its lowest level in five years. The abundance of *Calanus finmarchicus* copepods increased to near-normal levels in the western Gulf of St. Lawrence, decreased to below normal levels in the Cabot Strait and on the eastern and central Scotian Shelf, and showed little variation compared to 2017 on the northeast Newfoundland Shelf, the Grand Bank, and the western Scotian Shelf. The abundance of *Pseudocalanus* copepods decreased to below normal levels on the NL Shelf, but increased almost everywhere else in the NW Atlantic except in the Bay of Fundy where an unusually low negative anomaly was observed. Overall zooplankton biomass increased in 2018 compared to the time

series record lows of three previous years, but it remained below the climatology across the NW Atlantic except on the Labrador Shelf.

1. Introduction

We review biogeochemical oceanographic conditions on the Newfoundland and Labrador (NL) Shelf, Grand Banks (GB), Gulf of St. Lawrence (GSL), Scotian Shelf (SS), and Gulf of Maine (GM) during 2018, and reference earlier periods where data are available. Directed seasonal sampling on oceanographic sections by the Atlantic Zone Monitoring Program (AZMP[1]) and at coastal high frequency sampling stations by ships of opportunity provided reasonable spatial and temporal series coverage. Annual collection of standard variables (temperature, salinity, nutrients, chlorophyll, zooplankton abundance, biomass and composition) since 1998/1999 allows one to compare patterns of variation and trends among ecologically relevant chemical and biological indices in the Northwest (NW) Atlantic. Additional details on physical, chemical and biological oceanographic conditions in the NW Atlantic in 2018 and earlier years can be found in Blais et al. (2019), Colbourne et al. (2017), Galbraith et al. (2018), Hebert et al. (2018), Johnson et al. (2018), Pepin et al. (2017), Yashayaev et al. (2014).

2. Methods

Collections of standard AZMP variables are based on sampling protocols outlined by Mitchell *et al*. (2002). Observations for 2018 and earlier years presented in this document are based on seasonal surveys conducted during the spring through the autumn (typically March through December). The coastal high frequency sampling stations are typically sampled at twice monthly to monthly intervals during ice-free conditions. The location of the standard oceanographic sections and high frequency sampling stations are shown in Figure 1A.

Phytoplankton biomass was estimated from ocean colour satellite data collected by the Sea-viewing Wide Field-of-view Sensor (SeaWiFS; (https://oceancolor.gsfc.nasa.gov/SeaWiFS/), Moderate Resolution Imaging Spectroradiometer (MODIS) "Aqua" sensor (http://modis.gsfc.nasa.gov/), and the Visible-Infrared Imager Radiometer Suite (VIIRS) sensor (https://oceancolor.gsfc.nasa.gov/data/viirs-snpp/). The SeaWiFS time series began in September of 1997, MODIS data stream began in July 2002, and VIIRS availability is January 2012 to present. Satellite data do not provide information on the vertical structure of chlorophyll-*a* (chl *a*) pigments in the water column but do provide highly resolved (~1.5 km) data on their geographical distribution in surface waters on a large scale. 8-day composite images of chl *a* surface concentrations for the entire NW Atlantic (39-62.5° N Latitude 42-71° W Longitude) were routinely produced from SeaWiFS/MODIS/VIIRS data[2]. Basic statistics (mean, range, standard deviation, etc.) were extracted from the composites for selected subregions (Figure 1B) and used to calculate phytoplankton bloom indices. Time series of bloom magnitude, initiation, and duration from 1998 to 2018 were constructed by applying the calculation method developed by Zhai et al. (2011) to available satellite data from the SeaWiFS (1998-2007), MODIS (2008-2011), and VIIRS (2012-2018) sensors.

Standardized anomalies were used to summarize the variables selected to represent the state of nutrients and lower trophic levels in the NW Atlantic. Annual standardized anomalies were calculated for each variable by subtracting the mean of the long-term reference period (1998-2015 for satellite ocean colour data, and 1999-2015 for AZMP survey data) from the annual observation and by dividing the result by the standard deviation (SD) of the reference period ([observation – mean]/SD). Least square means derived from linear models with the fixed factors Year, Season and Station (standard oceanographic sections) or the fixed factor Year and Season (coastal high frequency sampling stations) applied to log transformed data (1+ln (x)) were used to calculate the standardized anomalies for the following parameters: 0-50 and 50-150 m integrated nitrate inventories; 0-100 m integrated chlorophyll *a* inventories; non-copepod, copepod, *Calanus finmarchicus*, and *Pseudocalanus* spp, abundances; zooplankton biomass. Annual standardized anomalies for Ocean colour satellite data (spring bloom magnitude, initiation, and duration) were calculated on raw data. The result of this standardization

[1] http://www.meds-sdmm.dfo-mpo.gc.ca/isdm-gdsi/azmp-pmza/index-eng.html
[2] http://www.bio.gc.ca/science/newtech-technouvelles/sensing-teledetection/index-en.php

yields a series of annual anomalies that illustrate departures from the long-term average conditions, or climatology, across the range of variables. The difference between a given year and the climatological mean represents the magnitude of that departure from the long-term reference period. Values near zero (e.g. ± 0.5 anomaly) indicate near normal conditions, positive values >0.5 indicate conditions above/later than the climatology, and negative values <0.5 indicate conditions below/earlier than the climatology. To estimate the large spatial scale trends in the chemical and biological observations across the NW Atlantic, a cumulated anomaly index was calculated for each sampling year by summing the annual anomalies of each AZMP oceanographic section and high frequency sampling station. In 2017, the reference period was extended to 1998/1999-2015, compared to 1998/1999-2010 for previous reports. Considering the non-stationary (or time-varying) state of the biological and chemical indices, extending the climatology to include recent years changes the mean against which observations are compared, which can shift the sign or magnitude of anomalies. While this issue must be kept in mind, the advantage of the extended reference period is to provide more relevant depictions of current system conditions and trends and place the observations in context with past levels of variability. Moreover, extending the reference period does not alter the general anomaly patterns for the time series. For the chemical-biological observations, the standard variables selected were: shallow (0-50 m integrated) and deep (50-150 m integrated) nitrate inventories; chlorophyll *a* (0-100 m integrated) inventories; spring bloom initiation, duration and magnitude indices; zooplankton abundance (total copepods, total non-copepods, *Calanus finmarchicus*, and *Pseudocalanus* spp.); and total zooplankton biomass.

3. Annual variability in nutrient, phytoplankton, and zooplankton conditions in the NAFO subareas

3.1 Nitrate and chlorophyll *a*

In 2018, shallow (0-50 m) nitrate inventories were below the climatology across the NW Atlantic except on the Bonavista section (3K) where nitrate anomaly was positive, and Southeastern GB (3LNO), Halifax (4W) and Browns Bank (4X) sections where nitrate inventories were near normal (Figure 2A). This represents a decrease in most regions compared to 2017, especially for the GB (3LNO), GSL (4RST) and the northern and central SS (4VW) (Figures 2A & 3A). The cumulated anomaly index indicates a general decreasing trend in shallow nitrate inventories across the NW Atlantic since 1999 with 2018 being the second lowest cumulated anomaly of the time series (Figure 3A). Deep (50-150 m) nitrate inventories were also below the climatology across the NW Atlantic except on the Bonavista (3K) and western GSL (4ST) sections and at the Shediac Valley (4T) high frequency sampling station (Figure 2B) where conditions were near normal. Deep nitrate inventories were generally lower than in 2017 on the NL Shelf, the GB, and in the GSL, but increased relative to the previous year on the SS (4VWX) (Figures 2B & 3B). The cumulated anomaly index has remained mostly below the climatology since 2010 with two consecutive record lows in 2017 and 2018 (Figure 3A). Deep nitrate inventories in 2018 may negatively impact primary production for 2019.

Chl *a* inventories in 2018 were near or above the climatology on the NL Shelf (2J3K) and the GB (3LNNMO) and in the GSL (4RST), near normal on the eastern and central SS (4VW), and below the climatology on the western SS and in the Bay of Fundy (4X) (Figure 4A). Compared to 2017, significant increases in chl *a* inventories were observed in the western GSL (4ST) while important decrease were observed at the Shediac Valley (4T) and Prince 5 (4X) high frequency stations (Figure 4A). Similarly to deep nitrate, the cumulated anomaly index for chl *a* has remained mostly below or near the climatology since 2010, but has increased to a positive value in 2018 (Figure 5A). Cumulated anomaly indices for chl *a*, shallow nitrate and deep nitrate (1-y lag) show similar overall decreasing trends for the 1999-2018 period along with periods of high interannual variability (e.g. 2007 and 2010). Trends in the chl *a* cumulated index generally matches the trends in either shallow and/or 1-y lag deep nitrate indices, except in 2018, when both nitrate indices were near the lowest of the time series. In 2018, the chl *a* index reached its highest level in ten years (Figure 5B). The timing of the spring bloom in relation to oceanographic sampling campaigns may have contributed to this observed difference.

3.2 Phytoplankton Spring Bloom

In 2018, the magnitude (total phytoplankton production) of the spring bloom based on remote sensing data was below the climatology on the Labrador Shelf (1F2HJ) and the western SS (no data available for the Lurcher Shoal subregion), mostly near normal on the GB (3LNOPs), and above the climatology in the St. Anthony Basin (3K), the Flemish Pass (3LM), the GSL and the eastern SS (3Pn4V) (Figure 6). Conditions were similar to 2017

on most of the GB (3LNOPs) and on the central and western SS and in the Bay of Fundy (4WX5Ze), but surface phytoplankton production markedly increased in the Cabot Strait (3Pn4Vn) and on the eastern SS (4Vs), and decreased in the western GSL (4S) (Figure 6 & 7). Comparison between 2017 and 2018 on the NL Labrador shelves (2HJ3K) was limited by insufficient satellite coverage in 2017 due to cloud and ice masking. Cumulated anomaly index had been fluctuating above and below the climatology during the 1999-2018 period but remained mostly negative since 2012 (Figure 7).

The initiation of the spring bloom in 2018 occurred earlier than normal in the GSL, near the long-term average on the GB (3LMNOPs), the SS (4VsWX) and on the Georges Bank (5Ze), and mostly later than normal on the NL Shelf (2HJ3KL) as well as in the Labrador Sea (1F2H) (Figure 8). On the GB (3LNOPs), anomalies shifted from positive (late blooms) in 2017, to near normal or negative (early blooms) in 2018. The early blooms observed on the central SS (4W) in 2017 were back to near normal in 2018 (Figure 8 & 9). Overall, the cumulated anomaly index indicates that bloom initiation in the NW Atlantic had been fluctuating between periods of early and late blooms since 1998 with no clear observable long-term trend (Figure 9).

The duration of the bloom in 2018 was mostly shorter than the climatology on the NL Shelf (2HJ3KL), near normal on the GB (3LNOPs), the SS (4VsWX) and Georges Bank (5Ze), and mostly longer than the climatology in the GSL (4RSTVn) (Figure 10). Compared to 2017, bloom duration markedly decreased in the Flemish Pass (3LM) and on the central SS (4W), but showed a general increase on the GB (Figure 10 & 11). Despite 1-4 y fluctuation cycles between shorter and longer blooms throughout the time series, the cumulated anomaly index shows a overall decreasing trend from 1998 to 2011, followed by a general increase in bloom duration (Figure 11).

3.3 Zooplankton Abundance and Biomass

In 2018, the abundance of non-copepod zooplankton organisms such as pelagic gastropods, larvaceans, chaetognaths, euphausiids, amphipods and invertebrate meroplanktonic larvae, was above the climatology on the northeast Newfoundland Shelf (3K) and the GB (3LNMO) with anomalies 3 to 4 times higher than the long-term average conditions along the Flemish Cap and the Southeastern GB sections. Non-copepod abundance was mainly near normal in the GSL and on the SS and Georges Bank (Figure 12A). Compared to 2017, abundance notably increased on the GB (3LNMO), and declined on the NL Shelf (2J3K) (Figures 12A & 13A). The cumulated anomaly index shows an overall increase in abundance from 2002 to a time series record high in 2016, followed by a decrease in abundance over the past two years on the SS and in the GSL (Figure 13A).

Copepod abundance remained above the long-term average conditions on the NL Shelf and the Grand Banks, near or above normal in the western GSL and the Estuary (4ST), and near or below normal on the SS and the Bay of Fundy (4VWX). (Figure 12B). Compared to 2017, copepod abundance declined on the NF Shelf (2J3K) and on the SS (3P4VWX), but generally increased in the GSL (4ST) (Figures 12B & 13B). The cumulated anomaly index indicate a general increase in copepod abundance in the NW Atlantic from 2002 to a time series record high in 2016, punctuated by a period of lower abundance from 2011 to 2013 (Figure 13B). Similarly to trend observed for non-copepod organisms, overall copepod abundance has decreased over the past two years on the SS and in the GSL (Figure 13B).

The abundance of the large grazing copepod *Calanus finmarchicus,* an important prey item preferentially selected by several planktivores and early life stage fish species, was generally near the long-term average on the NL Shelf (2J3K), the GB (3LMNO), and the GSL (4ST) in 2018, but was below the climatology in the Cabot Strait (3Pn4Vn) and on the SS (4VWX) (Figure 14A). A notable increase in *C. finmarchicus* abundance has been observed on the Labrador Shelf (2J), in the western GSL and Estuary (4ST), and on the southern SS (4X) compared to 2017 (Figures 14A & 15A). The cumulated anomaly index indicate an overall persistent decline in *C. finmarchicus* in the NW Atlantic since the mid-2010s (Figure 15A).

Pseudocalanus spp. are highly abundant, widely distributed, small epipelagic copepods also preferentially selected as prey items by planktivores and early life stage fish species. In 2018, the abundance of *Pseudocalanus* spp. was below the climatology on the NL Shelf (2J3K), on the central SS (4W) and at the high frequency sampling station Prince 5 in the Bay of Fundy (4X) where the negative anomaly was more than five times the

standard deviation for the long-term mean condition of the reference period (Figure 14B). Abundance was mainly near normal everywhere else except on the Southeastern GB (3LNO) and at the Shediac Valley (4T) high frequency sampling station where positive anomalies were observed (Figure 14B). Compared to 2017, abundance decreased on the NL Shelf (2J3K) but increased in the GSL (4ST) where anomalies shifted from negative to positive in most subareas (Figure 14B & 15B). The cumulated anomaly index indicates a slight increase in the overall abundance of *Pseudocalanus* spp. in 2018 after having decreased during two consecutive years following the 2015 record high (Figure 15B).

Zooplankton biomass in 2018 was below the climatology on the GB (3KLMNO) and in most of the GSL (4RST), and either near or below the climatology on the SS (4VWX) (Figure 16). Significant positive anomaly was only observed on the Labrador Shelf (2J) where, in 2017, the greatest negative anomaly among all subregions was observed. Zooplankton biomass generally increased across the NW Atlantic in 2018 compared to 2017 despite notable declines observed on the Southeastern GB (3LNO) and on the central and western SS (4WX) (Figure 16 &17). However, the cumulated anomaly index shows an overall decreasing trend in zooplankton biomass for the past 15 years in the NW Atlantic with the four lowest cumulated indices observed in the past four years (Figure 17). The changes in zooplankton biomass observed in recent years on the NL Shelf and GSL contributed significantly to the overall reduction compared to conditions on the SS.

4. Large-scale relationships between ocean chemistry, primary production and zooplankton abundance in the NW Atlantic

Pearson correlations applied to cumulated indices were used to investigate relationships among chemical (shallow and deep nitrate) and biological (chl *a* inventories, phytoplankton spring bloom, and zooplankton abundance and biomass) parameters in the NW Atlantic (Figure 18). Primary production in the ocean is mostly limited by nitrate availability. While nitrates in the upper water column actively fuel the development of ongoing phytoplankton blooms, nitrates in the deeper water column represent a pool of nutrients that will be available to primary producers the following year after being transported to the surface by vertical mixing during the winter months. Therefore, deep nitrate concentrations in a given year can be used as an indicator of primary production potential of following year. Significant positive correlation were observed between shallow (0-50 m) nitrate concentration and spring bloom initiation ($r = 0.65$, $p = 0.003$), between 1-y lag deep (50-150 m) nitrate and bloom duration ($r = 0.47$, $p = 0.043$), and between bloom magnitude and bloom duration ($r = 0.46$, $p = 0.046$) indicating that phytoplankton blooms tend to occur earlier when near-surface nitrate concentration is low, to last longer when previous year concentration of deep nitrate was high, and that longer blooms result in higher total primary production (Figure 18).

Zooplankton plays a critical role in the oceanic food chain and represents one of the main mechanisms of energy transfer from phytoplankton to higher trophic levels. Their abundance and distribution in marine ecosystems directly or incidentally impact the state of several ecologically and economically important stocks ranging from forage fish to whales. In the NW Atlantic, both abundance and biomass of zooplankton are dominated by copepods but other non-copepod organisms such as euphausiids, amphipods, pelagic gastropods, larvaceans, and chaetognaths are also of significant ecological importance. The abundance of copepod and non-copepods zooplankton were highly correlated ($r = 0.81$, $p < 0.001$) and similarities in the patterns of variation between theses two taxonomic group throughout the time series may indicate large-scale community response to changing environmental conditions in the NW Atlantic. The negative correlation between copepod abundance and zooplankton biomass ($r = -0.70$, $p = 0.001$) can be explained by a shift in zooplankton community size-structure. The general increase in total copepod abundance observed throughout the time series (Figure13B) was mostly driven by an increase in the abundance of small, highly abundant copepod taxa, including *Pseudocalanus* spp. (Figure 15B), concurrent with an overall decrease in the abundance of significantly larger, however less numerous, taxa such as *C. finmarchicus* (Figure 15A) resulting in a net decrease in total zooplankton biomass. This also explains the negative correlation ($r = -52$, $p = 0.022$) between *C. finmarchicus* and copepod abundance as well as the positive correlation ($r = 0.83$, $p < 0.001$) between *C. finmarchicus* and zooplankton biomass (Figure 18). Both *C. finmarchicus* abundance ($r = 0.50$, $p = 0.029$) and zooplankton biomass ($r = 0.58$, $p = 0.010$) were positively correlated with spring bloom magnitude highlighting the potential cascading effects of primary production on higher trophic levels. *Pseudocalanus* spp. is one of the most

numerous copepods in the study area and a good indicator of the general pattern of variation in total copepod abundance as indicated by the positive correlation ($r = 0.61$, $p = 0.006$) between the two. In the NW Atlantic, zooplankton biomass is mainly controlled by copepods, which can account for up to 90% of total zooplankton abundance. Consequently, non-copepod organisms have a lesser impact on zooplankton biomass and significant relationship observed between the abundance of non-copepod organisms and zooplankton biomass ($r = -0.85$, $p < 0.001$), *C. finmarchicus* abundance ($r = -0.78$, $p = <0.001$), and *Pseudocalanus* spp. abundance ($r = 0.5$, $p = 0.029$) can be attributed to the similitude in the variation patterns of abundance between copepod and non-copepod organisms.

5. Biological oceanographic highlights in 2018

- Nitrate inventories in the upper (0-50 m) and lower (50-150 m) water column were near or below the 1999-2015 climatology throughout the NW Atlantic with respectively the second lowest, and the lowest overall concentrations of the 20-y time series.
- The chlorophyll *a* inventories inferred from the seasonal AZMP oceanographic surveys and fixed stations were mostly above the climatology on the NL Shelf, the Grand Banks, and the GSL, and near or below normal on the SS.
- The magnitude (total production) of the spring bloom was mainly near or below the climatology across the NW Atlantic despite some highly productive blooms in the St. Anthony Basin (3K), the Flemish Pass (3LM), and the Cabot Strait and eastern SS (4V).
- Initiation of the phytoplankton spring bloom occurred earlier than normal in the GSL, and later than normal in the Labrador Sea and on the NL Shelf.
- The duration of the spring bloom was, on average, near the 1999-2015 climatology with slightly shorter blooms on the NL Shelf, and some markedly longer blooms in the GSL.
- The abundance of non-copepod zooplankton was significantly above normal on the northeast Newfoundland Shelf (3K) and the GB (3LNO) compared to the 1999-2015 climatology with notable increase on GB compared to 2017.
- Despite an overall decrease in total copepods in the NW Atlantic, the general abundance pattern remained unchanged compared to 2017 with positive anomalies on the NL Shelf and the Grand Banks, and negative anomalies on the SS.
- The abundance of *Calanus finmarchicus* showed an overall increase compared to 2017, but remained below the climatology almost everywhere in the NW Atlantic.
- The abundance of *Pseudocalanus* copepods also generally increased across the study area but markedly decreased in the Bay of Fundy (4X).
- The abundance of *Pseudocalanus* spp. copepods reflected the general pattern of change in small copepod abundance, whereas abundance of the larger copepod *Calanus finmarchicus* reflected the general pattern of change in total zooplankton biomass.
- Zooplankton biomass increased compared to 2017 but remained below normal across most of the survey area with the fourth lowest overall biomass of the 20-y time series after 2015, 2016 and 2017.

Acknowledgements

We thank the staff at Fisheries and Oceans Canada's Northwest Atlantic Fisheries Centre (NWAFC) Biological and Physical Oceanography Section, Bedford Institute of Oceanography (BIO), Ocean and Ecosystem Sciences Division (OESD), and the Maurice-Lamontagne Institute (IML), Pelagic and Ecosystem Science Branch, for their acquisition, quality control and archiving of the data. We also wish to thank the efforts of the many scientific assistants and science staff at the Northwest Atlantic Fisheries Centre in St, John's, the Bedford Institute of Oceanography, the Maurice-Lamontagne Institute, and the St. Andrews Biological Station and CCGS Teleost, CCGS Hudson, and the Coriolis II officers and crew for their invaluable assistance at sea. The expertise of the Atlantic Reference Center in St. Andrews, and of Jackie Spry at BIO, was crucial to the completion of this work. Special thanks to Gina Doyle, Shannah Rastin, Devyn Ramsay, Brittany Pye, Jennifer Higdon, Steve Snook and Ryan Doody for their important contribution to data collection, to Jean-Yves Couture, Marie-France Beaulieu, Caroline Lebel, Isabelle St-Pierre, and Caroline Lafleur from IML for preparation and standardization of the phytoplankton and zooplankton data. The data used in this report would not be available without the work of François Villeneuve and his AZMP team (Rémi Desmarais, Marie-Lyne Dubé, Line McLaughlin, Roger Pigeon, Michel Rousseau, Félix St-Pierre, Liliane St-Amand, Sonia Michaud, Isabelle St-Pierre, David Leblanc, and Caroline Lafleur) in organizing and carrying out AZMP surveys in the Gulf region and analyzing samples. We thank Jeff Spry and Kevin Pauley for providing data from the Shediac Valley station and BIO's remote sensing unit for the composite satellite images.

References

Blais, M., Galbraith, P.S., Plourde, S., Scarratt, M., Devine, L. and Lehoux, C. 2019. Chemical and Biological Oceanographic Conditions in the Estuary and Gulf of St. Lawrence during 2017. DFO Can. Sci. Advis. Sec. Res. Doc. 2019/009. iv + 56 pp.

Colbourne, E., Holden, J., Snook, S., Han, G. Lewis, S., Senciall, D., Bailey, W., Higdon, J. and Chen, N. 2017. Physical Oceanographic Conditions on the Newfoundland and Labrador Shelf during 2016. DFO Can. Sci. Advis. Sec. Res. Doc. 2017/079. v + 50 p.

Galbraith, P.S., Chassé, J., Caverhill, C., Nicot, P., Gilbert, D., Lefaivre, D. and Lafleur, C. 2018. Physical Oceanographic Conditions in the GSL in 2017. DFO Can. Sci. Advis. Sec. Res. Doc. 2018/050. v + 91 p.

Hebert, D., Pettipas, R., Brickman, D., and Dever, M. 2018. Meteorological, Sea Ice and Physical Oceanographic Conditions on the Scotian Shelf and in the Gulf of Maine during 2016. DFO Can. Sci. Advis. Sec. Res. Doc. 2018/016. v + 53 p.

Johnson, C., Devred, E., Casault, B., Head, E., and Spry, J. 2018. Optical, Chemical, and Biological Oceanographic Conditions on the Scotian Shelf and in the Eastern Gulf of Maine in 2016. DFO Can. Sci. Advis. Sec. Res. Doc. 2018/017. v + 58 p.

Mitchell, M.R., Harrison, G., Pauley, K., Gagné, A., Maillet, G., Strain, P. 2002. Atlantic Zone Monitoring Program Sampling Protocol. Canadian Technical Report of Hydrography and Ocean Sciences 223, 23 pp.

Pepin, P., Maillet, G., Fraser, S., Doyle, G., Robar, A., Shears, T., and Redmond, G. 2017 Optical, chemical, and biological oceanographic conditions on the Newfoundland and Labrador Shelf during 2014-2015. DFO Can. Sci. Advis. Sec. Res. Doc. 2017/009. v + 37 p.

Yashayaev, I., Head, E.J.H., Azetsu-Scott, K., Ringuette, M., Wang, Z., Anning, J., and Punshon, S. 2014. Environmental Conditions in the Labrador Sea during 2013. DFO Can. Sci. Advis. Sec. Res. Doc. 2014/105. v +35 p.

Zhai, L., Platt, T., Tang, C., Sathyendranath, S., and Hernández Walls, R. 2011. Phytoplankton phenology on the SS. – ICES Journal of Marine Science, 68: 781–791.

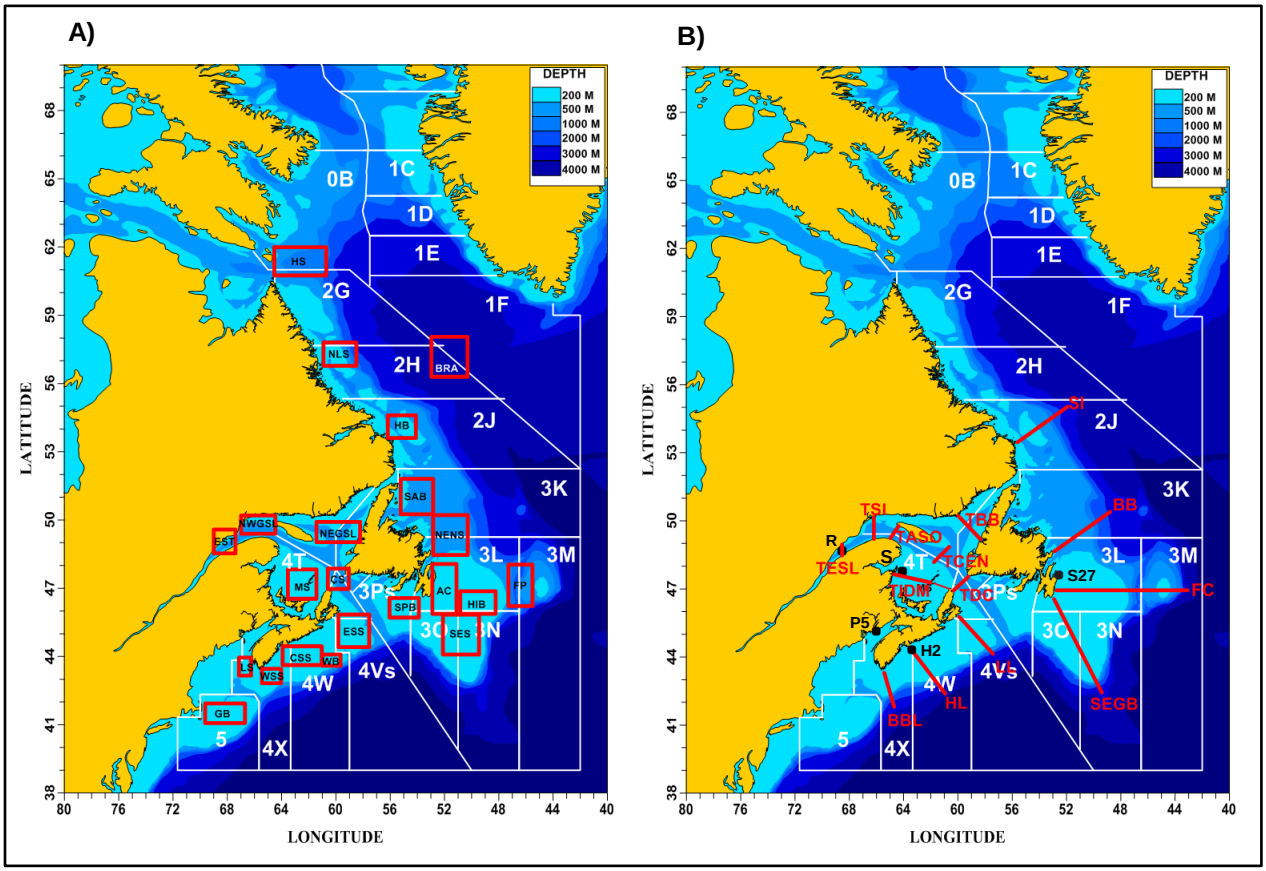

Figure 1. **(**A) Location of the statistical subregions used to calculate phytoplankton spring bloom indices (magnitude, peak timing and duration of spring bloom) derived from satellite ocean colour data (BRA=Bravo, HS=Hudson Strait, NLS=northern Labrador Shelf, HB=Hamilton Bank, SAB=St. Anthony Basin, NENS=northeast Newfoundland Shelf, FP=Flemish Pass, HIB=Hibernia, AC=Avalon Channel, SES=southeast Shoal, SPB=Green-St. Pierre Bank, NEGSL=northeast GSL, NWGSL=western GSL, EST = Estuary, MS=Magdalen Shallows, CS=Cabot Strait, ESS=eastern SS, WB=Western Bank, CSS=central SS, WSS=western SS, LS=Lurcher Shoal, GB=Georges Bank. (B) Location of primary Atlantic Zone Monitoring Program (AZMP) oceanographic sections (red lines: SI=Seal Island, BB=Bonavista Bay, FC=Flemish Cap, SEGB=Southeastern Grand Bank, TBB+TCEN+TDC=eastern GSL, TESL+TSI+TASO=Western GSL, TIDM=Southern GSL, LL=Louisbourg Line, HL=Halifax Line, BBL=Brown Bank Line), and coastal high frequency sampling stations (black dots: S27=Station 27, R=Rimouski, S=Shediac Valley, H2=Halifax 2, P5=Prince 5) from which chemical (nitrate) and biological (chlorophyll *a* and zooplankton) data were collected.

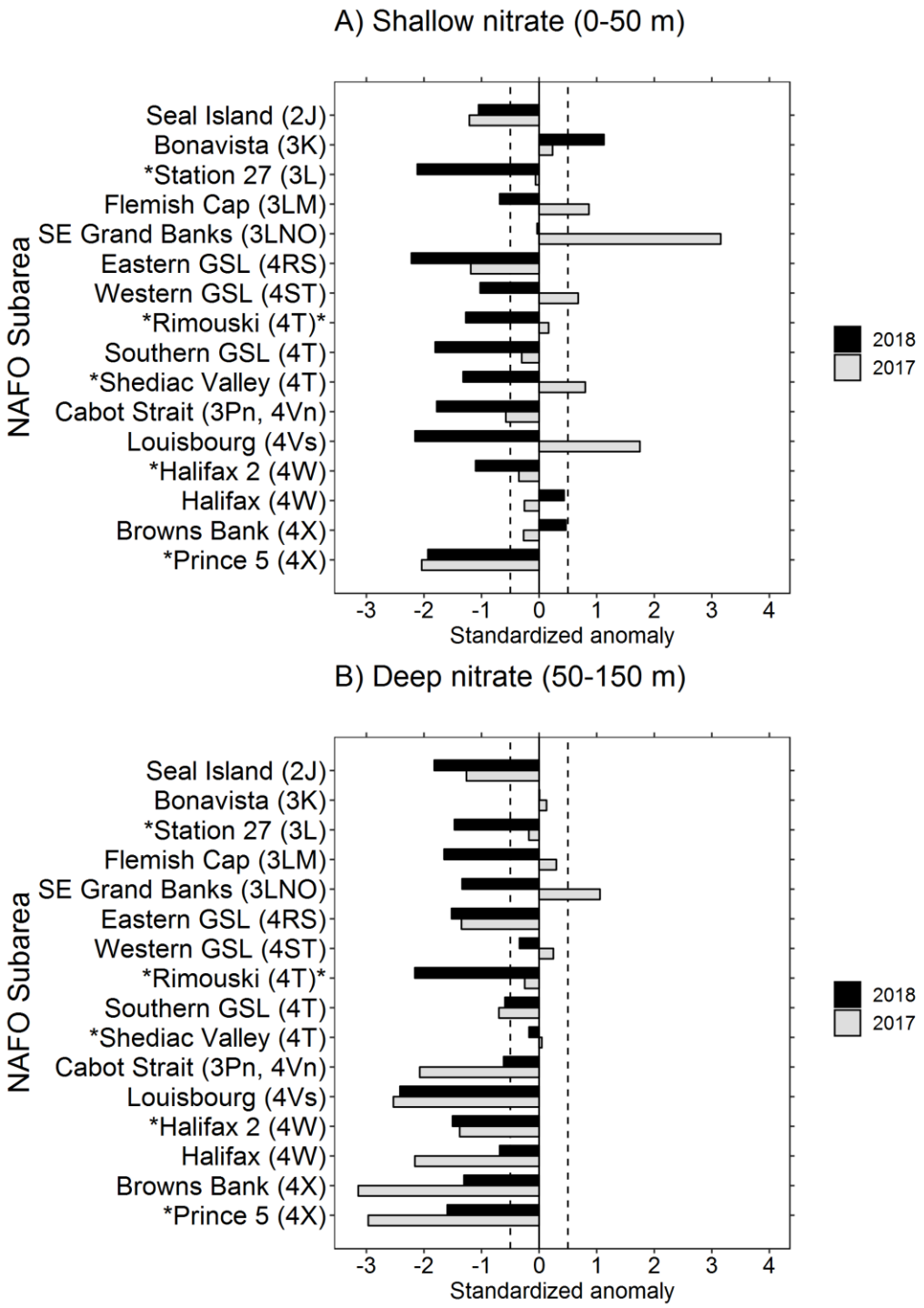

Figure 2. Summary of anomalies for nitrate inventories in (A) the upper [0-50 m] water column, and (B) the lower [50-150m] water column from AZMP oceanographic sections and high frequency sampling stations during the 2017 and 2018 AZMP surveys. Anomalies within -0.5 and 0.5 (vertical dashed lines) are regarded as normal conditions relative to the long-term average. NAFO Subareas are sorted by latitude from north (top) to south (bottom). High frequency sampling stations are identified with an asterisk (*).

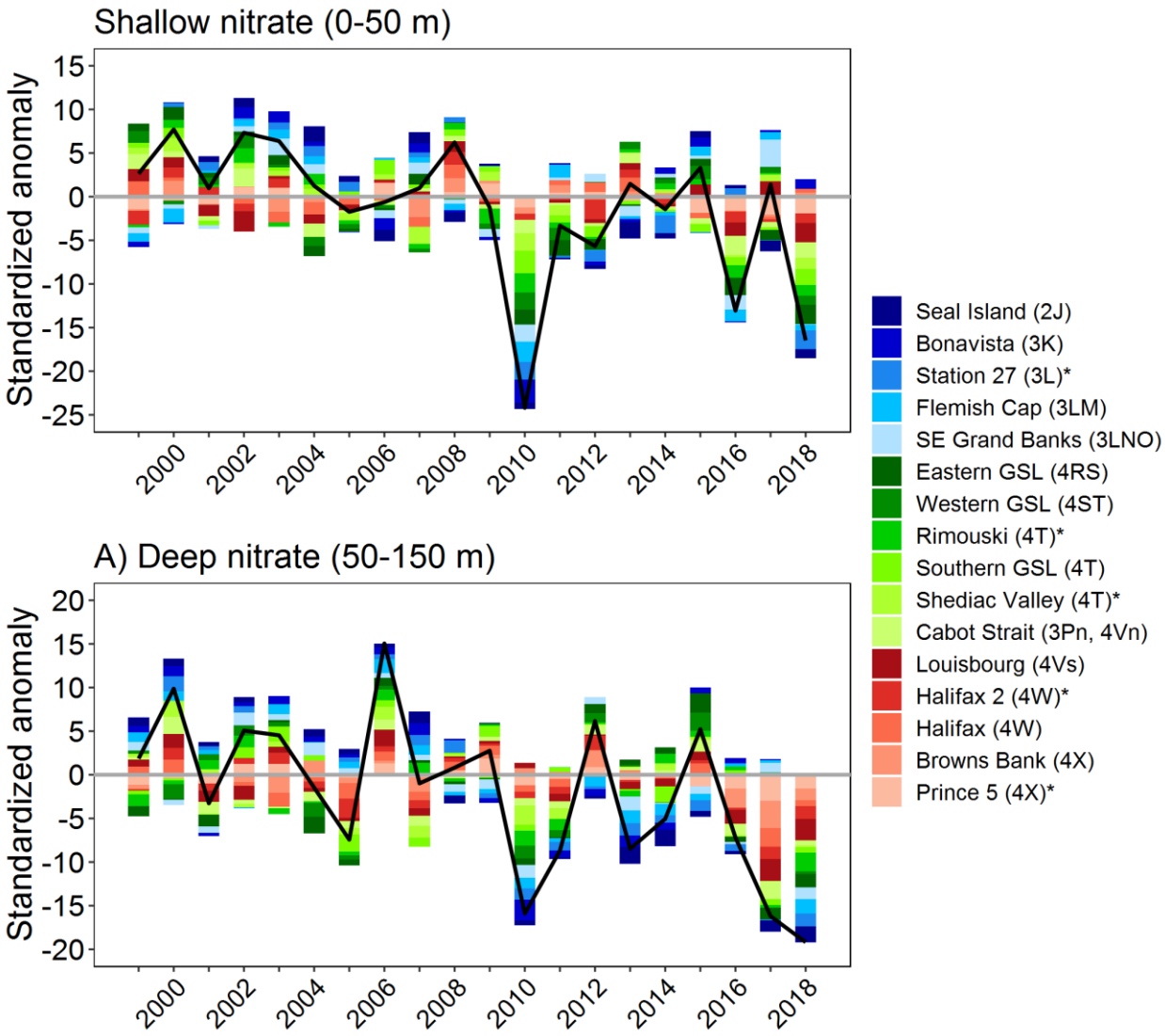

Figure 3. Time series of (A) shallow (0-50m) and (B) deep (50m-150m) nitrate inventory anomalies for different AZMP oceanographic sections and high frequency sampling stations for the period 1999-2018. Blue shades are associated to the NL Shelf and the Grand Banks, green shades to the Gulf of St. Lawrence, and red shades to the Scotian Shelf. The solid black line is the cumulated anomaly index, i.e. the sum of anomalies across all NAFO subareas in a given year. High-frequency sampling stations are identified with an asterisk (*)

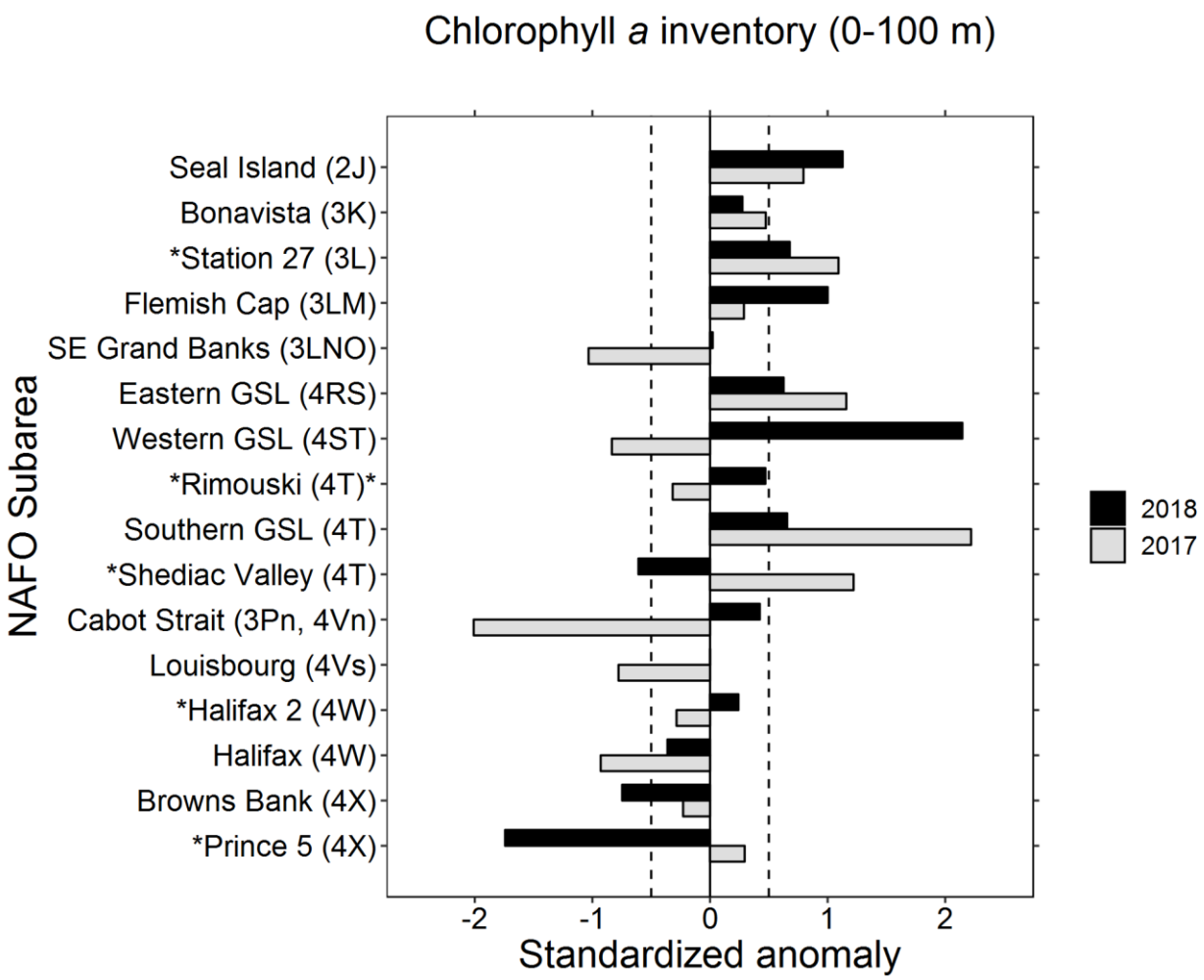

Figure 4. Summary of chlorophyll *a* inventory (0-100 m) from AZMP oceanographic sections and high frequency sampling stations during the 2017 and 2018 AZMP surveys. Anomalies within -0.5 and 0.5 (vertical dashed lines) are regarded as normal conditions relative to the long-term average. NAFO Subareas are sorted by latitude from north (top) to south (bottom). High frequency sampling stations are identified with an asterisk (*).

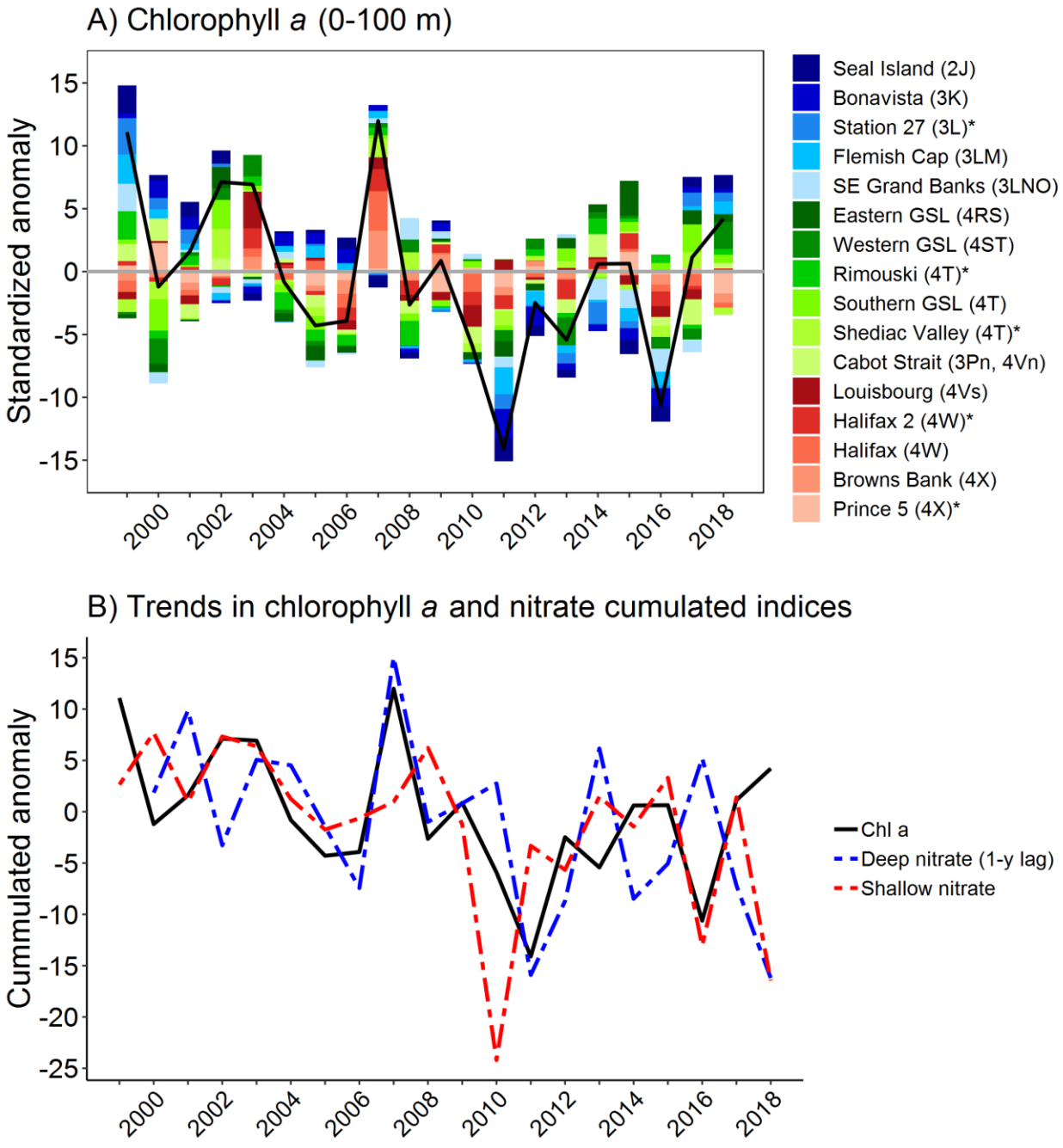

Figure 5. (A) Anomaly time series for chlorophyll *a* (0-100 m) inventories from different AZMP oceanographic sections and high frequency sampling stations for period 1999-2018. Blue shades are associated to the NL Shelf and the Grand Banks, green shades to the Gulf of St. Lawrence, and red shades to the Scotian Shelf. The solid black line is the cumulated anomaly index, i.e. the sum of anomalies across all NAFO subareas in a given year. High-frequency sampling stations are identified with an asterisk (*). (B) Comparison between cumulated anomaly indices of shallow nitrate (0-50m), 1-y lag deep nitrate (50-150m), and chlorophyll *a* for the 1999-2018 period.

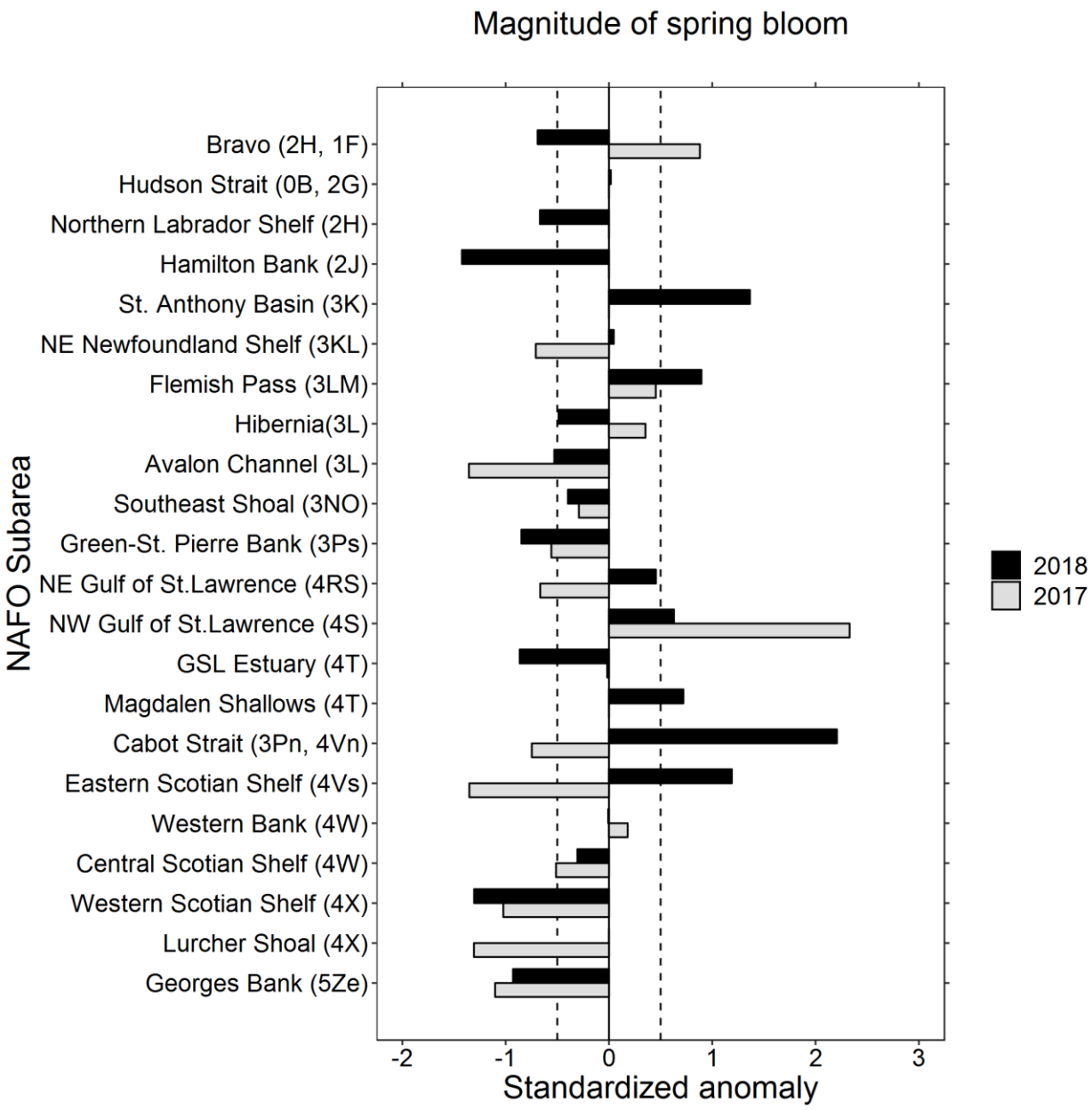

Figure 6. Summary of anomalies for the magnitude of the phytoplankton spring bloom within predefined subregions in the NW Atlantic in 2017 an 2018. Standardized anomalies were calculated over a 1998-2015 reference period using surface chlorophyll *a* concentration estimates derived from 8-d composite ocean colour satellite images. Anomalies within -0.5 and 0.5 (vertical dashed lines) are regarded as normal conditions relative to the long-term average. Subregions are sorted by latitude from north (top) to south (bottom) with the exception of the Labrador Sea subregion (Bravo) at the top.

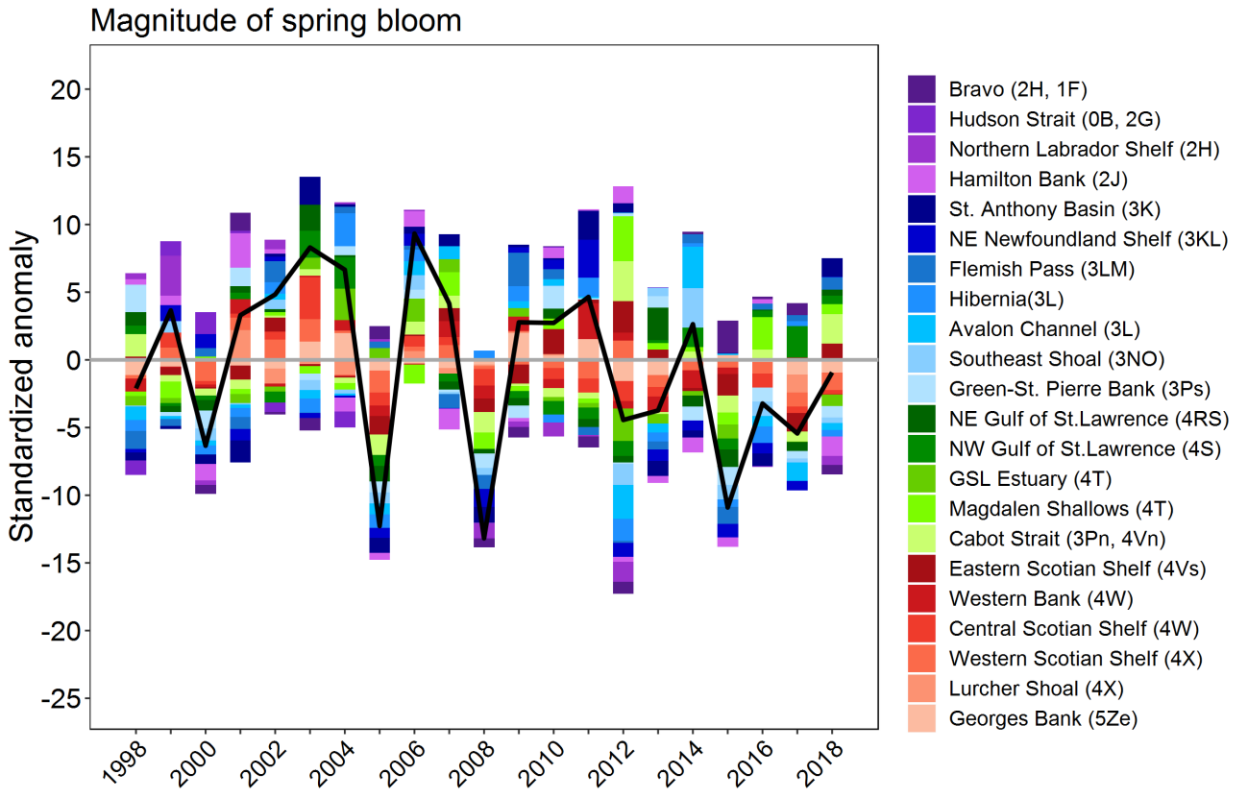

Figure 7. Anomaly time series for the magnitude of the phytoplankton spring bloom within predefined subregions in the NW Atlantic for the period 1998-2018. Standardized anomalies were calculated over a 1998-2015 reference period using surface chlorophyll *a* concentration estimates derived from 8-d composite ocean colour satellite images. Purple shades are associated to the Labrador Sea and the Labrador shelf, blue shades to the Newfoundland shelf and the Grand Banks, green shades to the Gulf of St. Lawrence, and red shades to the Scotian Shelf and the Gulf of Maine. The solid black line is the cumulated anomaly index, i.e. the sum of anomalies across all NAFO subareas in a given year.

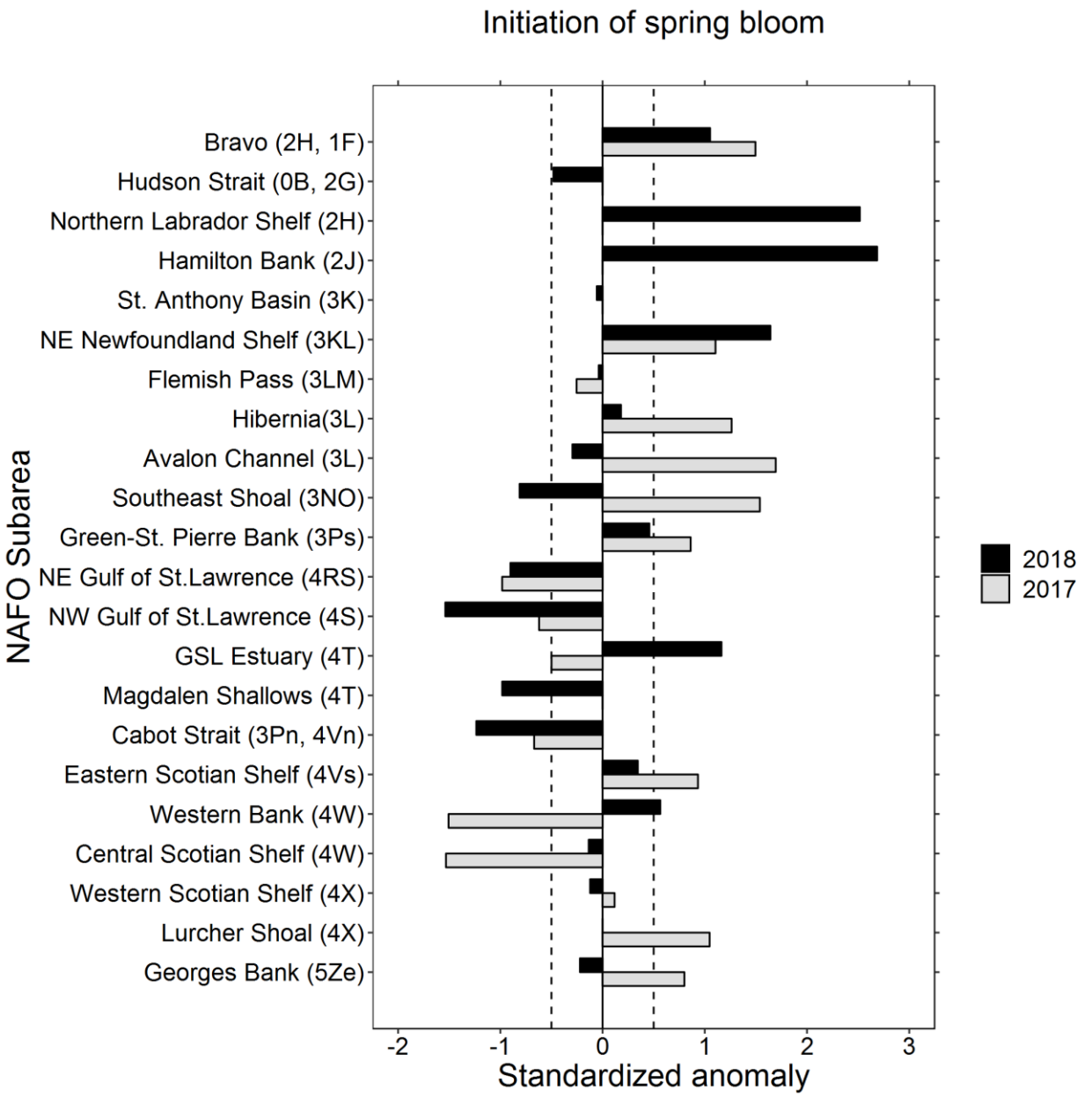

Figure 8. Summary of anomalies for the initiation of the phytoplankton spring bloom within predefined subregions in the NW Atlantic in 2017 an 2018. Standardized anomalies were calculated over a 1998-2015 reference period using surface chlorophyll *a* concentration estimates derived from 8-d composite ocean colour satellite images. Anomalies within -0.5 and 0.5 (vertical dashed lines) are regarded as normal conditions relative to the long-term average. Subregions are sorted by latitude from north (top) to south (bottom) with the exception of the Labrador Sea subregion (Bravo) at the top.

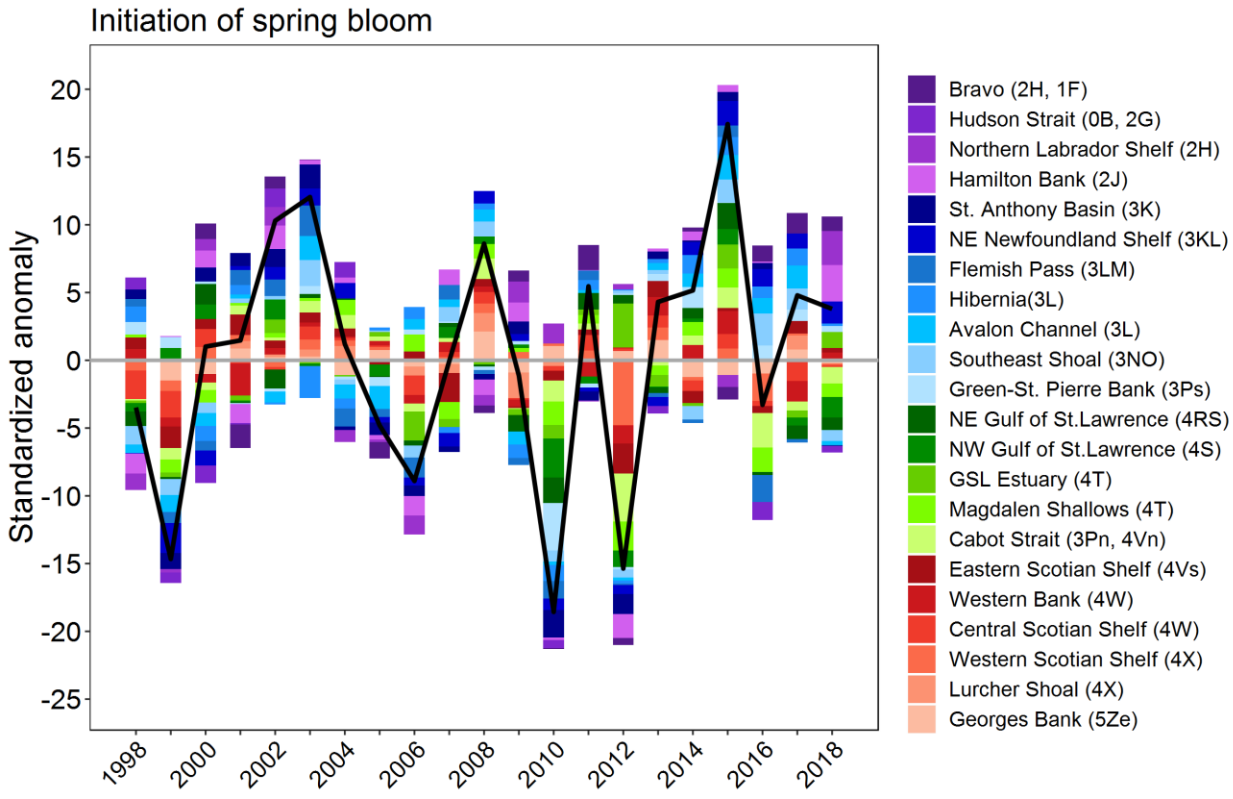

Figure 9. Anomaly time series for the initiation of the phytoplankton spring bloom within predefined subregions in the NW Atlantic for the period 1998-2018. Standardized anomalies were calculated over a 1998-2015 reference period using surface chlorophyll *a* concentration estimates derived from 8-d composite ocean colour satellite images. Purple shades are associated to the Labrador Sea and the Labrador shelf, blue shades to the Newfoundland shelf and the Grand Banks, green shades to the Gulf of St. Lawrence, and red shades to the Scotian Shelf and the Gulf of Maine. The solid black line is the cumulated anomaly index, i.e. the sum of anomalies across all NAFO subareas in a given year.

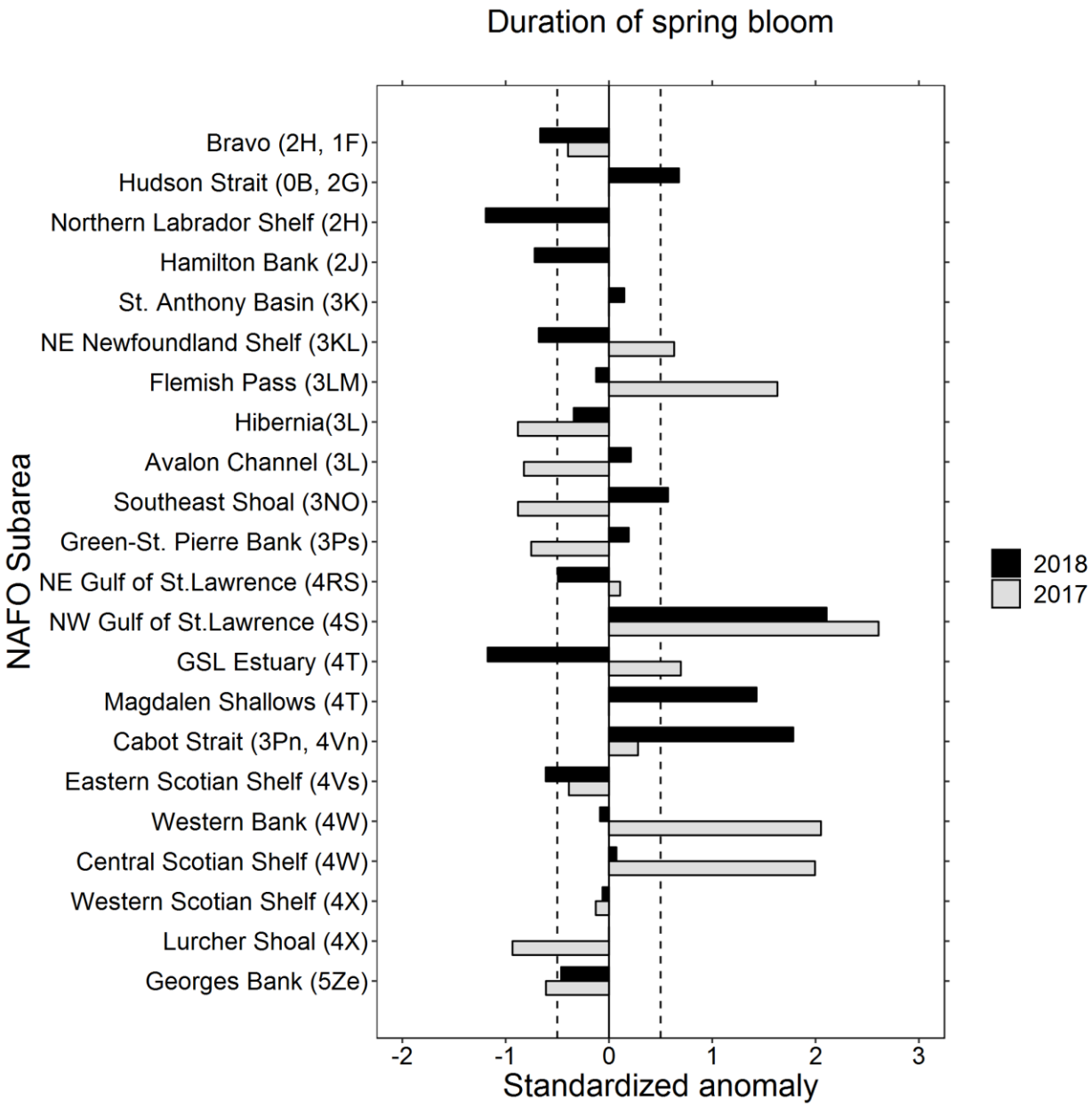

Figure 10. Summary of anomalies for the duration of the phytoplankton spring bloom within predefined subregions in the NW Atlantic in 2017 an 2018. Standardized anomalies were calculated over a 1998-2015 reference period using surface chlorophyll *a* concentration estimates derived from 8-d composite ocean colour satellite images. Anomalies within -0.5 and 0.5 (vertical dashed lines) are regarded as normal conditions relative to the long-term average. Subregions are sorted by latitude from north (top) to south (bottom) with the exception of the Labrador Sea subregion (Bravo) at the top.

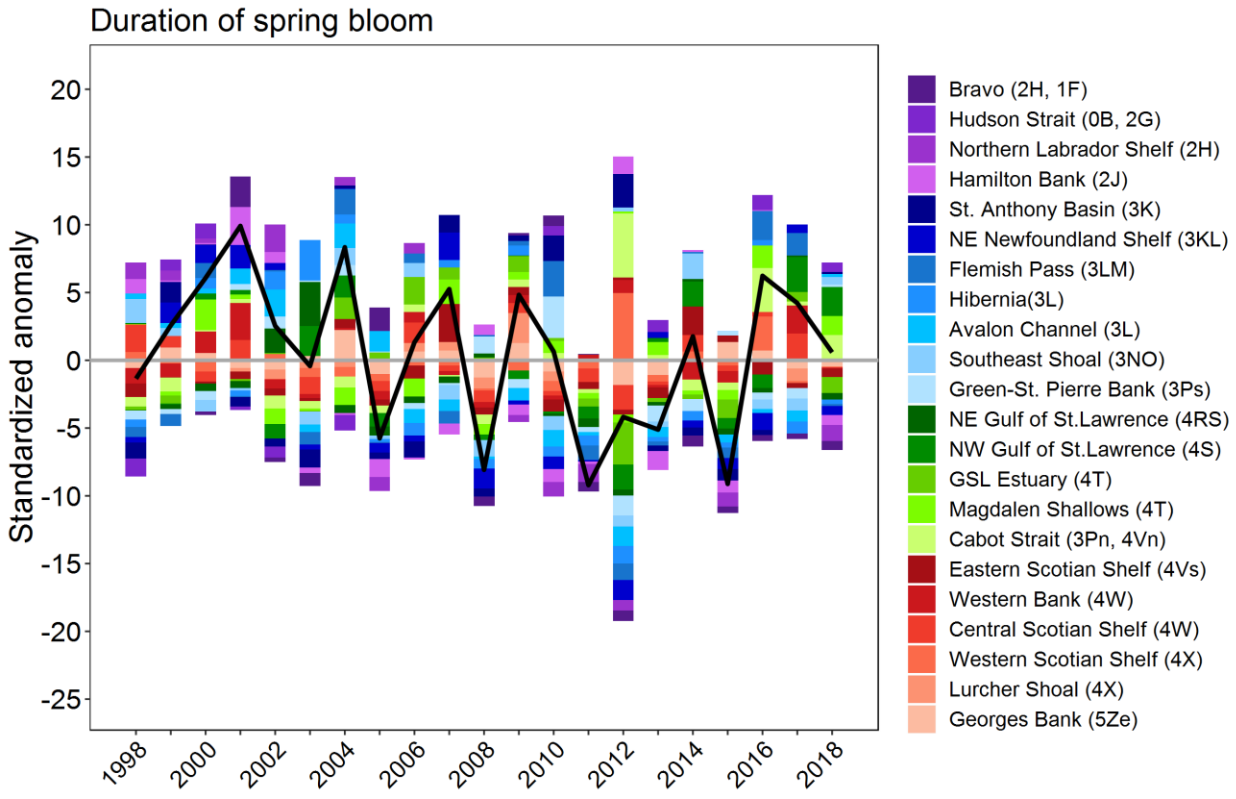

Figure 11. Anomaly time series for the duration of the phytoplankton spring bloom within predefined subregions in the NW Atlantic for the period 1998-2018. Standardized anomalies were calculated over a 1998-2015 reference period using surface chlorophyll *a* concentration estimates derived from 8-d composite ocean colour satellite images. Purple shades are associated to the Labrador Sea and the Labrador shelf, blue shades to the Newfoundland shelf and the Grand Banks, green shades to the Gulf of St. Lawrence, and red shades to the Scotian Shelf and the Gulf of Maine. The solid black line is the cumulated anomaly index, i.e. the sum of anomalies across all NAFO subareas in a given year.

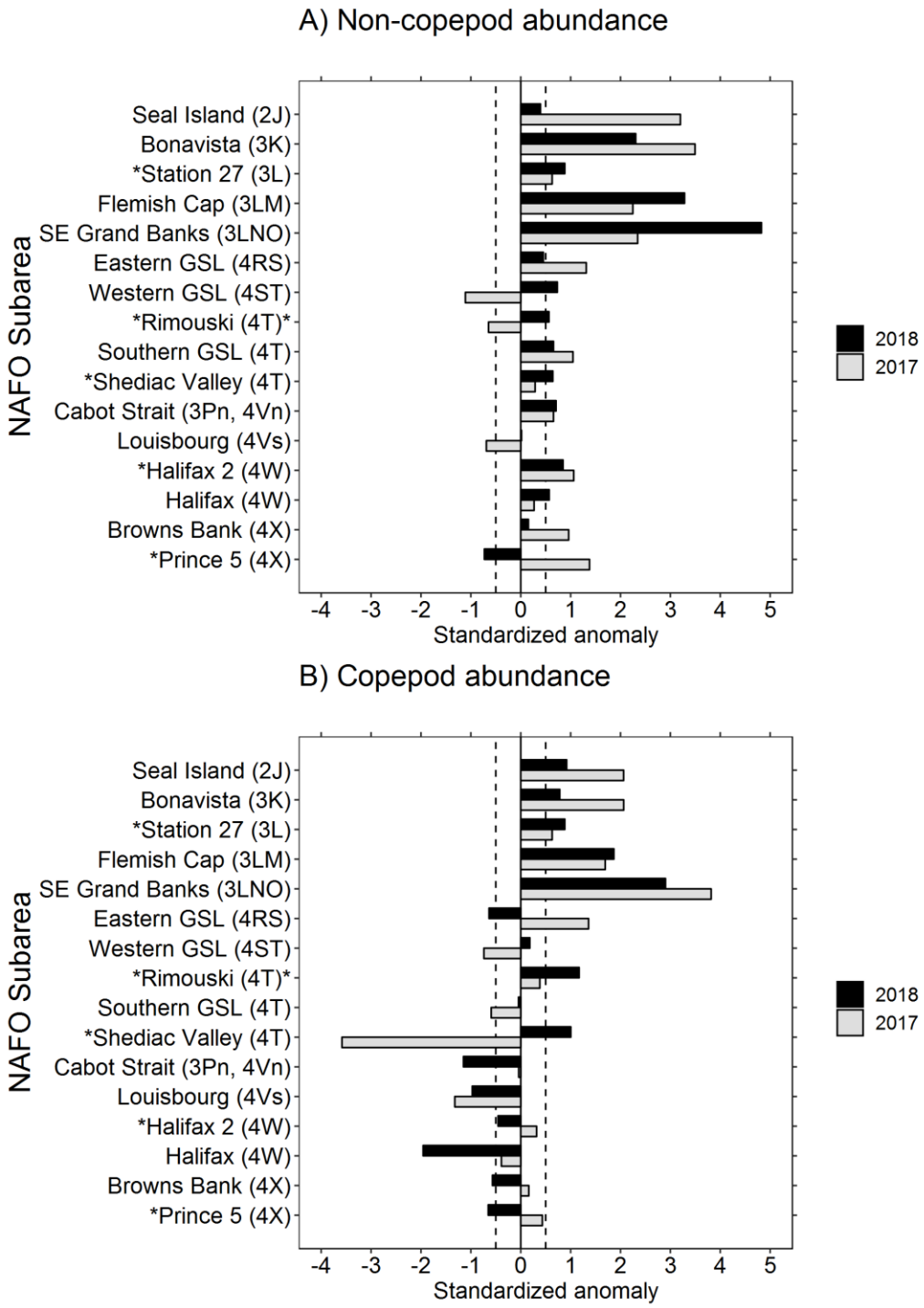

Figure 12. Summary of anomalies for the abundance of (A) non-copepod, and (B) copepod from AZMP oceanographic sections and high frequency sampling stations during the 2017 and 2018 AZMP surveys. Anomalies within -0.5 and 0.5 (vertical dashed lines) are regarded as normal conditions relative to the long-term average. NAFO Subareas are sorted by latitude from north (top) to south (bottom). High frequency sampling stations are identified with an asterisk (*).

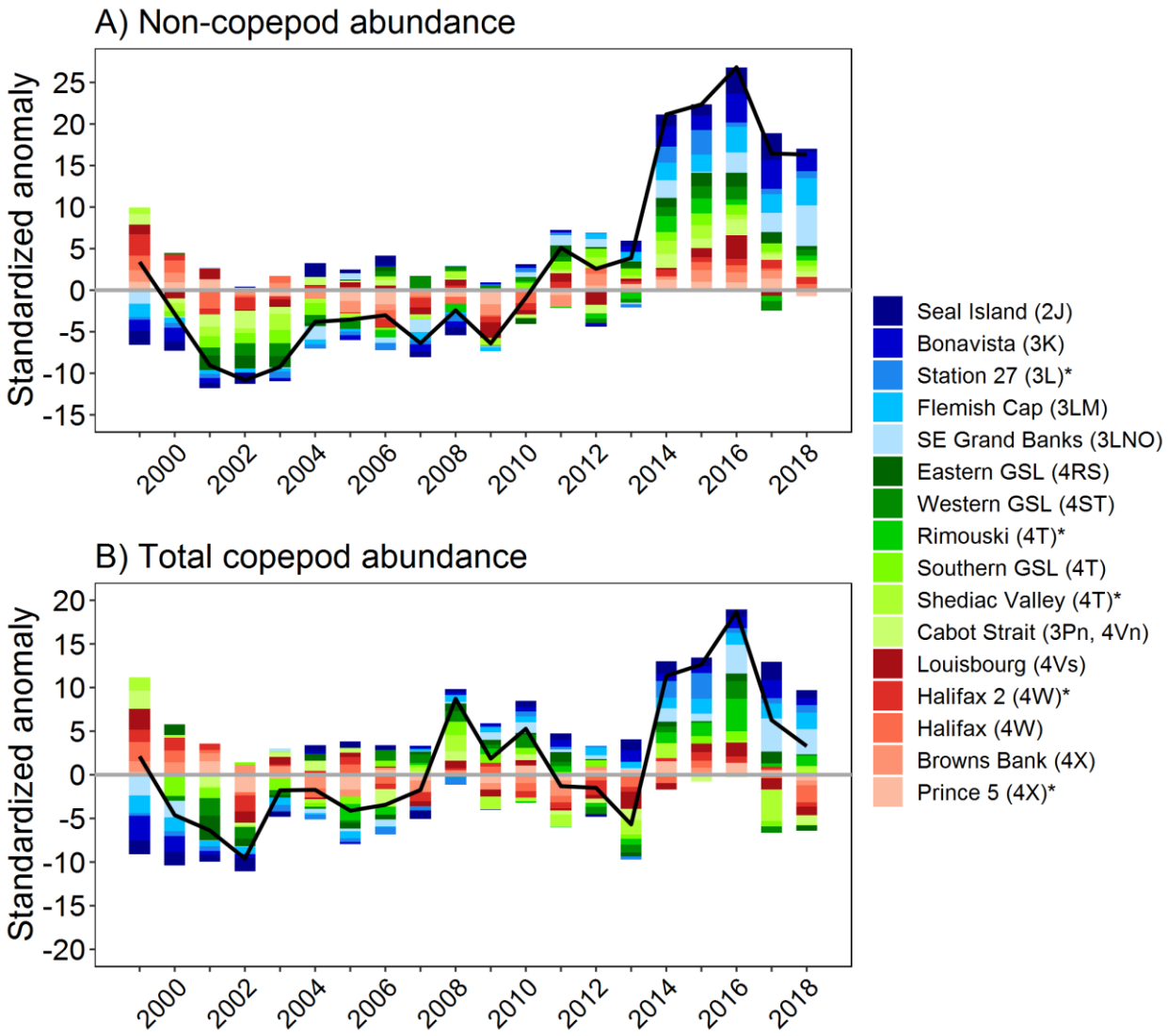

Figure 13. Anomaly time series for the abundance of (A) non-copepod, and (B) copepod zooplankton from different AZMP oceanographic sections and high frequency sampling stations for the period 1999-2018. Blue shades are associated to the NL Shelf and the Grand Banks, green shades to the Gulf of St. Lawrence, and red shades to the Scotian Shelf. The solid black line is the cumulated anomaly index, i.e. the sum of anomalies across all NAFO subareas in a given year. High-frequency sampling stations are identified with an asterisk (*)

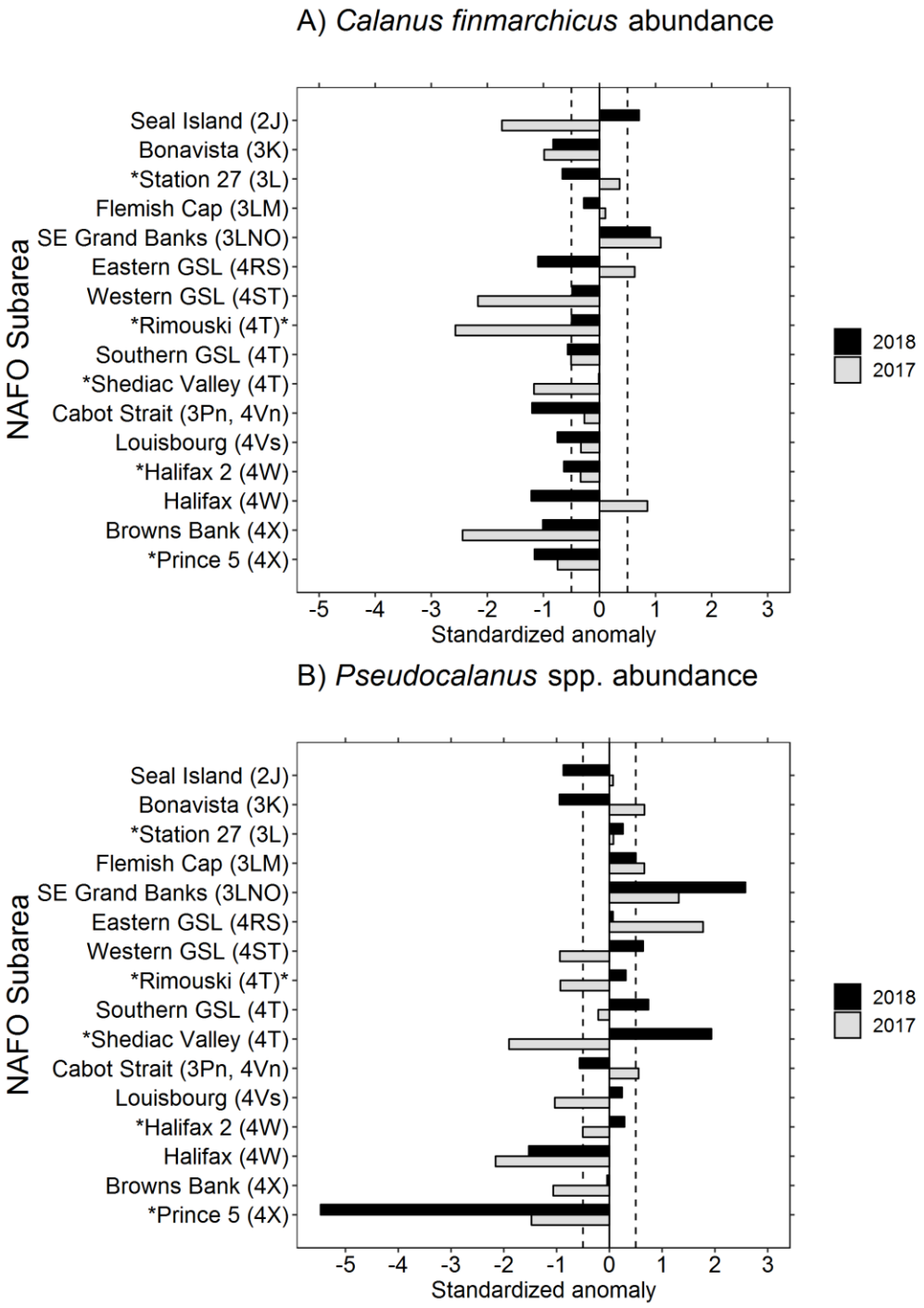

Figure 14. Summary of anomalies for the abundance of (A) *Calanus finmarchicus*, and (B) *Pseudocalanus* spp. copepods from AZMP oceanographic sections and high frequency sampling stations during the 2017 and 2018 AZMP surveys. Anomalies within -0.5 and 0.5 (vertical dashed lines) are regarded as normal conditions relative to the long-term average. NAFO Subareas are sorted by latitude from north (top) to south (bottom). High frequency sampling stations are identified with an asterisk (*).

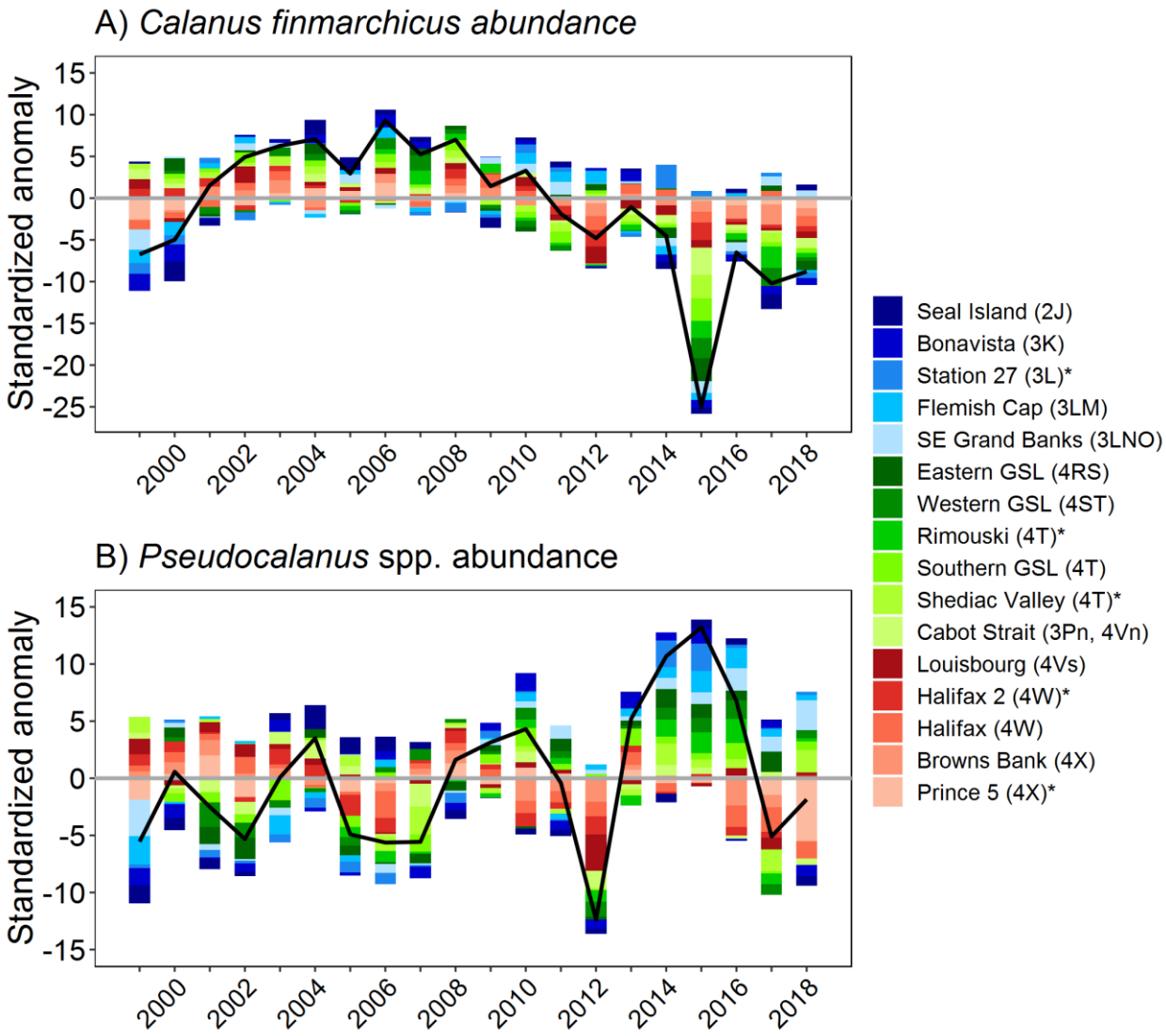

Figure 15. Anomaly time series for the abundance of (A) *Calanus finmarchicus* (B) *Pseudocalaanus* spp. copepods from different AZMP oceanographic sections and high frequency sampling stations for the period 1999-2018. Blue shades are associated to the NL Shelf and the Grand Banks, green shades to the Gulf of St. Lawrence, and red shades to the Scotian Shelf. The solid black line is the cumulated anomaly index, i.e. the sum of anomalies across all NAFO subareas in a given year. High-frequency sampling stations are identified with an asterisk (*)

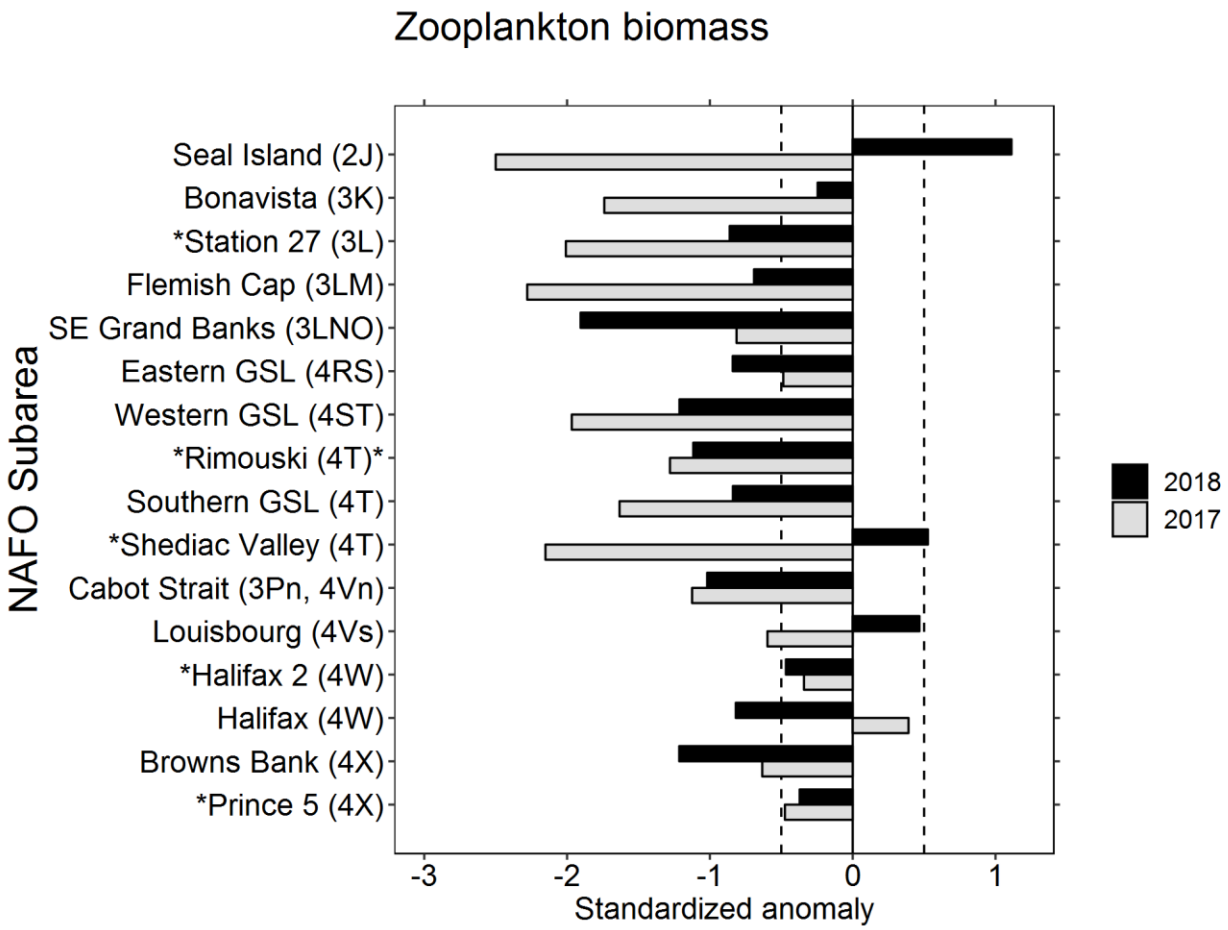

Figure 16. Summary of anomalies for total zooplankton biomass from AZMP oceanographic sections and high frequency sampling stations during the 2017 and 2018 AZMP surveys. Anomalies within -0.5 and 0.5 (vertical dashed lines) are regarded as normal conditions relative to the long-term average. NAFO Subareas are sorted by latitude from north (top) to south (bottom). High frequency sampling stations are identified with an asterisk (*).

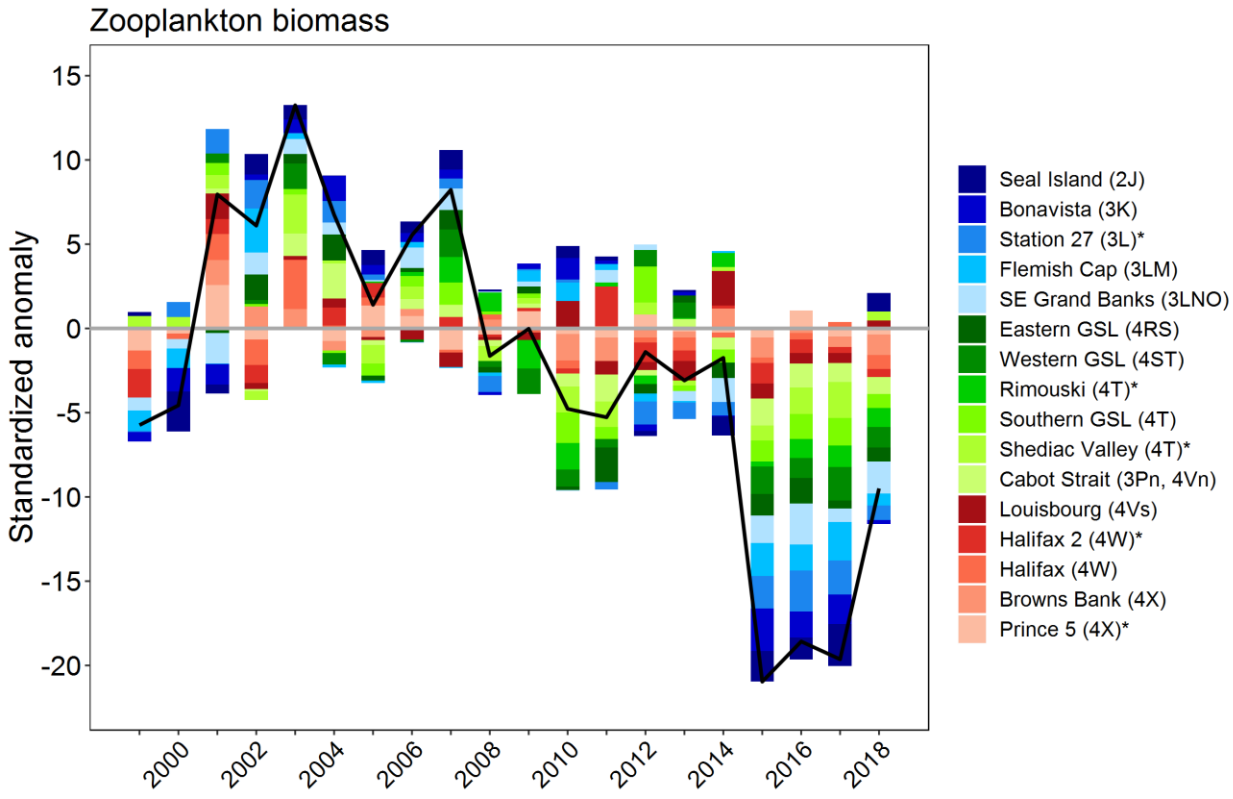

Figure 17. Anomaly time series for the total biomass of zooplankton from different AZMP oceanographic sections and high frequency sampling stations for the period 1999-2018. Blue shades are associated to the NL Shelf and the Grand Banks, green shades to the Gulf of St. Lawrence, and red shades to the Scotian Shelf. The solid black line is the cumulated anomaly index, i.e. the sum of anomalies across all NAFO subareas in a given year. High-frequency sampling stations are identified with an asterisk (*)

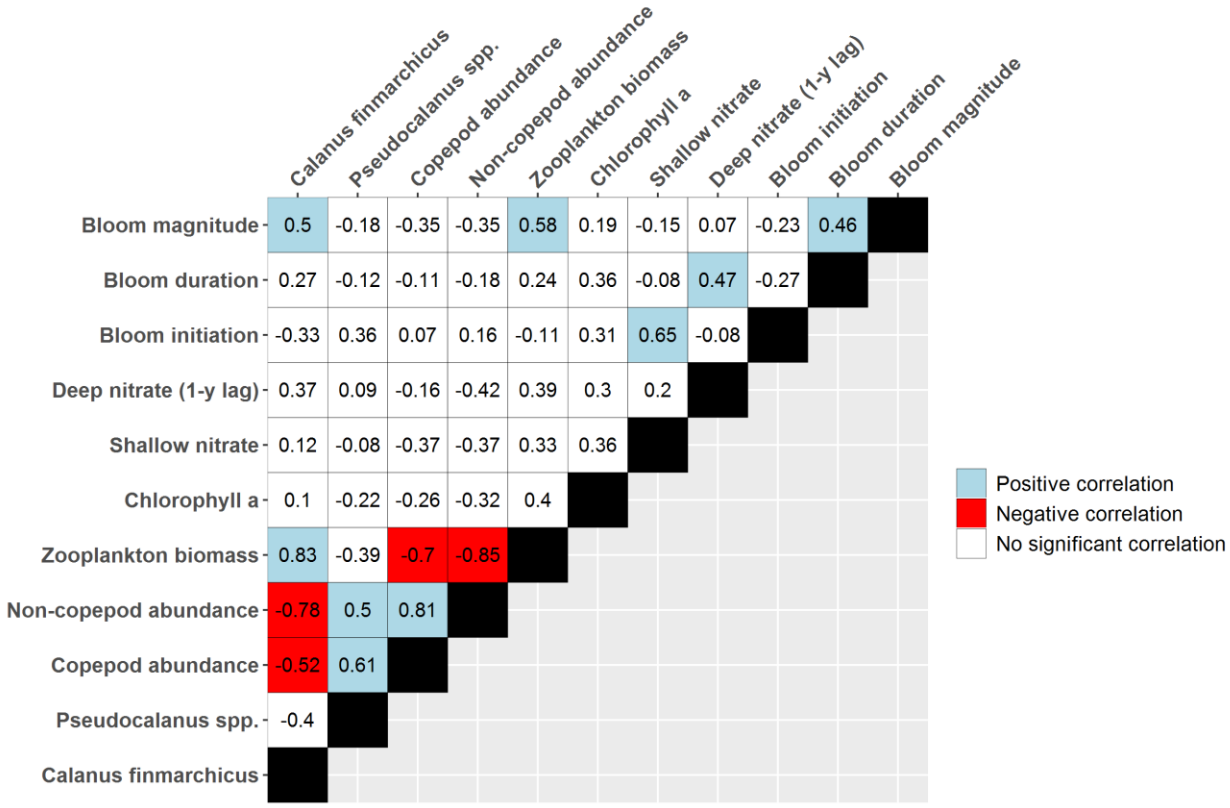

Figure 18. Summary of the relationship between chemical (nitrate) and biological (phytoplankton spring bloom and zooplankton abundance and biomass) cumulated anomaly indices for the period 1999-2018. Blue cells indicate significant positive correlation, red cells indicate significant negative correlation, and white cells indicate non-significant correlations. Numbers in cells are Pearson correlation coefficients (r). Significance level for Pearson correlation tests was α=0.05.